Heterogeneous Fenton's-like catalyst potentiation of hydrogen peroxide disinfection: an investigation into mechanisms of action.

SEWELL, S.L., OWEN, L., LAIRD, K., HUDDERSMAN, K.D. and WALSH, S.E.

2023

Journal of Applied Microbiology, 2023, 134, 1–9
https://doi.org/10.1093/jambio/lxad017
Advance access publication date: 16 February 2023
Research Article

JOURNAL OF APPLIED MICROBIOLOGY
OXFORD UNIVERSITY PRESS

Heterogeneous Fenton's-like catalyst potentiation of hydrogen peroxide disinfection: an investigation into mechanisms of action

Samantha L. Sewell[1], Lucy Owen[1], Katie Laird[1], Katherine D. Huddersman[1], Susannah E. Walsh[1,2,*]

[1]School of Pharmacy, Faculty of Health and Life Sciences, De Montfort University, Leicester, LE1 9BH, UK
[2]School of Pharmacy and Life Sciences, Robert Gordon University, Aberdeen, AB10 7AQ, UK

*Corresponding author. School of Pharmacy and Life Sciences, Robert Gordon University, Aberdeen, AB10 7AQ, UK. Tel: +44 (0)1224 262501; E-mail: susannah.walsh@rgu.ac.uk

Abstract

Aims: This study aimed to establish the mechanisms of action (MOA) of a novel surface-functionalized polyacrylonitrile (PAN) catalyst, which was previously shown to have potent antimicrobial activity in conjunction with hydrogen peroxide (H_2O_2).

Methods and results: Bactericidal activity was determined using a disinfectant suspension test. The MOA was investigated by measuring the loss of 260 nm absorbing material, membrane potential, permeability assays, analysis of intra- and extracellular ATP and pH, and tolerance to sodium chloride and bile salts.
The catalyst lowered sub-lethal concentrations of H_2O_2 from 0.2 to 0.09%. H_2O_2 ± 3 g PAN catalyst significantly ($P \leq 0.05$) reduced sodium chloride and bile salt tolerance, suggesting the occurance of sublethal cell membrane damage. The catalyst significantly increased ($P \leq 0.05$) N-Phenyl-l-Napthylamine uptake (1.51-fold) and leakage of nucleic acids, demonstrating increased membrane permeability. A significant ($P \leq 0.05$) loss of membrane potential (0.015 a.u.), coupled with pertubation of intracellular pH homeostasis and depletion of intracellular ATP, suggests potentiation of H_2O_2-mediated cell membrane damage.

Conclusions: This is the first study to investigate the catalyst's antimicrobial mechanism of action, with the cytoplasmic membrane being a target for cellular injury.

Significance of impact of the study

Understanding the MOA by which the catalyst potentiates H_2O_2 could lead to the optimization of concentrations and contact times needed for disinfection in a wide range of settings.

Keywords: mechanism of action, hydrogen peroxide, fenton, disinfection, polyacrylonitrile

Introduction

Hydrogen peroxide (H_2O_2) is a widely used biocide in the food and healthcare sectors, for example, in the disinfection of surfaces, medical devices, or contact lenses (McEvoy and Rowan 2019, Gabriel et al. 2021, Jones and Joshi 2021). Gram-negative bacteria appear to be more sensitive to H_2O_2 than Gram-positive bacteria, with recently published research demonstrating that higher concentrations of H_2O_2 were required for bactericidal efficacy against *Listeria monocytogenes* and *Staphylococcus aureus* (1.0–3.0%), compared to *Salmonella enteritidis* and *Escherichia coli* (0.1–0.5%) (Výrostková et al. 2020). H_2O_2 was also demonstrated to possess biocidal activity against *S. aureus* and *Pseudomonas aeruginosa* biofilms (Lineback et al. 2018), while spores generally require higher concentrations and/or longer contact times than vegetative bacterial cells (Boateng et al. 2011). For example, *Escherichia coli* and *S. aureus* were reduced by 4.76–5.37 $\log_{10}$ within 60 min of exposure to 0.2–0.5% H_2O_2, respectively, while 7.5% H_2O_2 reduced *Bacillus subtilis* and *Bacillus cereus* spores by 2.80–4.22 $\log_{10}$ in 120 min (Boateng et al. 2011).

A novel surface-functionalized polyacrylonitrile (PAN) catalyst (Huddersman and Walsh 2013) has been previously demonstrated to significantly increase the activity of hydrogen peroxide (H_2O_2) against a range of organisms, including Gram-positive and Gram-negative bacteria, spores, mycobacteria, and *Acanthamoeba*, at both reduced concentrations and contact times compared to H_2O_2 alone (Boateng et al. 2011, Price et al. 2013, Kilvington and Winterton 2017). H_2O_2 is a low-molecular-weight molecule that is able to pass through the porins of Gram-negative bacteria and through the cytoplasmic membrane of other microorganisms (Möller et al. 2019, Feng et al. 2020). As a reactive oxygen species, H_2O_2 causes oxidative damage (Jones and Joshi 2021), primarily through the production of highly reactive hydroxyl radicals (OH•) (Collin 2019). OH• is produced from H_2O_2 during the Fenton reaction, which is catalysed by iron (Walter et al. 2020) and other transition metals (Cheng et al. 2018). Previous published studies have suggested that H_2O_2 exhibits two concentration-dependent modes of action. At low H_2O_2 concentrations, bacterial cell death is considered to be caused by DNA damage associated

Received: July 6, 2022. **Revised:** October 10, 2022. **Accepted:** February 15, 2023

with Fenton's reaction occurring with intracellular free iron. Whereas at higher concentrations (>10 mM), such as those used for disinfection, H_2O_2 toxicity is less well understood but hypothesized to be caused by damage to a range of targets (Linley et al. 2012, Agashe and Kuzminov 2022), for example, proteins and enzymes by oxidation of thiol groups (Möller et al. 2019). The cell membrane is thought to be an important target for H_2O_2, leading to increased membrane permeability, loss of membrane function, and cellular death (Möller et al. 2019, Kim and Lee 2021). The mechanisms of action (MOA) of the PAN catalyst and H_2O_2 system are, like H_2O_2 alone, not fully understood (Price et al. 2013). The PAN catalyst is impregnated with ferric sulphate resulting in Fe(III) chelated to amidoxime, amidrazone, and acylhydrazone groups (Ishtchenko et al. 2003) as well as potentially amide and carboxylic acid groups. This suggests that OH• may be involved in the MOA of the PAN catalyst and H_2O_2 system in a Fenton-like reaction mechanism, which is the second step in the Haber–Weiss Fenton reaction mechanism involving Fe(II) (Meyerstein 2021). The aim of this study was to investigate the MOA, the type of sub-lethal injury, and the repair mechanisms cells use to recover after exposure to sub-lethal concentrations of H_2O_2 in conjunction with the PAN catalyst {PAN catalyst [Fe] = 16.8 mg g^{-1} (0.30 mmol g^{-1})}.

Materials and methods

Microorganisms

Escherichia coli ATCC 10 536 was routinely cultured using tryptone soya agar (Oxoid, Basingstoke, UK) supplemented with 0.6% w/v yeast extract (TSAYE) for 24 h at 37°C followed by tryptone soya broth (Oxoid, Basingstoke, UK) with 0.6% w/v yeast extract (TSBYE) for 16–18 h at 37°C unless otherwise specified. For downstream studies, cells were pelleted at 3000 g for 20 min and re-suspended in sterile distilled water at 9 $\log_{10}$ colony forming units (CFU) mL^{-1}.

Determination of sub-lethal concentrations of hydrogen peroxide

The highest concentration of H_2O_2 ± 3 g PAN catalyst with no significant effect on microbial viability (sublethal concentration) was determined using an adapted BS EN 1040:2005 disinfectant suspension test (British Standards Institution 2005) as previously described (Price et al. 2013). Catalase (0.015% w/v) was employed as a neutralizer to prevent antimicrobial carryover during enumeration and was validated as non-toxic and effective against H_2O_2; 3 g of PAN catalyst alone was also verified as non-toxic (Supplementary Table S1). To determine sub-lethal concentrations, *E. coli* was treated with various concentrations (0.05–0.4% w/v) of H_2O_2 ± 3 g PAN catalyst in 75 ml sterile distilled water for 15, 30, and 60 min. At each contact time, 1 mL of the test solution was added to 9 mL of catalase and incubated at room temperature for 5 min ± 10 s. Samples were then serially diluted in distilled water and 20 μL spot-plated onto TSAYE in triplicate using the Miles and Misra method (Miles and Misra 1938). Plates were incubated at 37°C for 24 h prior to enumeration.

Sub-lethal injury of *E. coli* by H_2O_2 ± PAN catalyst

The type of sub-lethal bacterial cell injury was determined using an adapted method from Somolinos et al. (2009). *E. coli* was treated for up to 60 min with the pre-determined sub-lethal concentration for H_2O_2 alone (0.2% w/v) or H_2O_2 ± 3 g PAN catalyst (0.09% w/v) in 75 ml sterile distilled water before neutralization in catalase. Treated samples were plated onto TSAYE plus 4% w/v sodium chloride (Fisher Scientific, UK) (TSAYE + SC) and TSAYE plus 0.2% w/v bile salts (Sigma-Aldrich, UK) (TSAYE + BS) to evaluate cytoplasmic and outer membrane damage, respectively. These levels of sodium chloride and bile salts were previously determined as the maximum non-inhibitory concentrations for non-treated cells (Supplementary Material, Table S2). *E. coli* was enumerated following incubation at 37°C for 48 h. Incubation at 48 h had no significant effect on bacterial cell counts compared to 24 h on TSAYE.

Controls of water alone and 3 g of PAN catalyst in water were included.

Membrane permeability

Changes in membrane permeability in *E. coli* upon exposure to 0.2% H_2O_2 ± 3 g of PAN catalyst were determined using an adapted method from Fisher and Phillips (2009). An overnight culture of *E. coli* in brain heart infusion (BHI) broth was washed twice in sterile distilled water (20 min centrifugation; 6738 g) and resuspended in sterile distilled water to an OD_{600} of 1.0 (8.28 ± 0.18 log10 CFU mL^{-1}). Cells were diluted 1:1 (v/v) in HEPES buffer with 40 μmol L^{-1} N-Phenyl-l-Napthylamine (NPN) and the pH adjusted to 7.2 using 1 mol L^{-1} hydrochloric acid (HCl) and 1 mol L^{-1} sodium hydroxide (NaOH).

The uptake of NPN was then measured (excitation 355 nm; emission 405 nm) immediately using a fluorescence spectrometer (Perkins Elmer, UK). After the fluorescence stabilized, 0.2% w/v H_2O_2 ± 3 g of PAN catalyst leachate were added, and changes in fluorescence were monitored for 30 min. NPN uptake, measured by an increase in fluorescence, was used to infer increased membrane permeability.

Nucleic acid leakage

The nucleic acid loss from cells was measured using an adapted method from Carson et al. (2002) and Chen and Cooper (2002). An overnight culture of *E. coli* in BHI broth was re-suspended in distilled water as described above to 8.90 ± 0.15 $\log_{10}$ CFU mL^{-1}. An aliquot (7.5 ml) of bacterial suspension was added to 67.5 ml 0.2% w/v H_2O_2 ± 3 g of PAN catalyst for 60 min. Samples of treatment solution were taken at 10-min intervals and syringe filtered through a 0.2 μm membrane (Fisher, UK) before OD_{260nm} was measured using a UV-Vis spectrophotometer. Controls were *E. coli* treated with water only.

Intracellular and extracellular ATP

The intra- and extracellular ATP concentrations were determined using an adapted method from Fisher and Phillips (2009). An overnight culture of *E. coli* in BHI broth was re-suspended in 25 mmol L^{-1} potassium phosphate (Fisher Scientific, UK) buffer (pH 7) to an OD_{600} of 1.0. Cells were energized by adding 0.5% w/v glucose (Fisher Scientific, UK), and after 6 min, 0.2% w/v H_2O_2 ± 3 g of PAN catalyst were added. Aliquots (200 μL) were taken every 2 min after the addition of glucose for a total of 14 min and added to microcentrifuge tubes (1.5 mL) containing 200 μL silicon oil on top of 100 μL trichloroacetic acid (10% w/v) in 2 mmol L^{-1} Tris-EDTA pH 7.2 buffer (Sigma Aldrich, UK). The samples

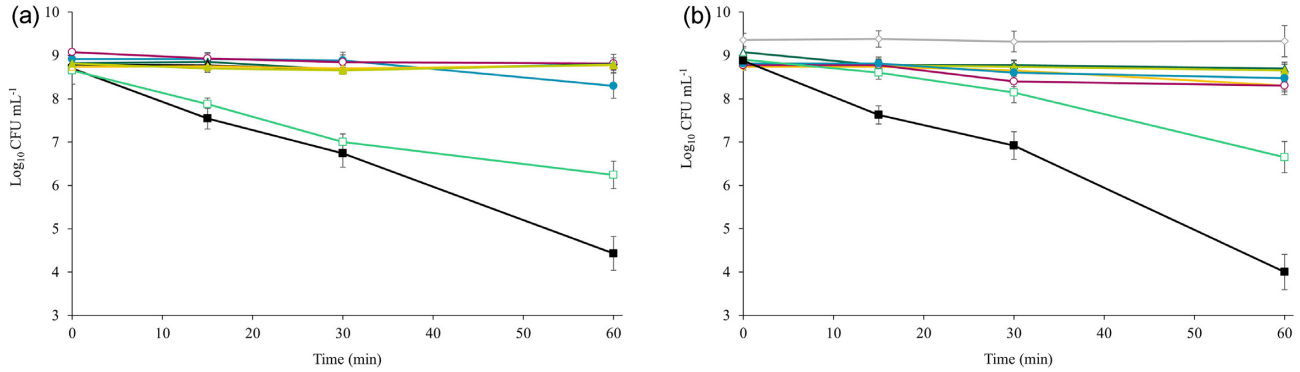

Figure 1. Determination of sub-lethal concentrations of (a) H_2O_2 and (b) H_2O_2 in the presence of 3 g of PAN catalyst against 8.90 $\log_{10}$ CFU mL^{-1} *E. coli* (mean, $n = 3 \pm$ SD) log10 CFU/ml recovery. (a) ■ 0.40% w/v H_2O_2; □ 0.30% w/v • 0.20% w/v; ○ 0.10% w/v; ▲ 0.09% w/v; △ 0.08% w/v; ♦ 0.07% w/v; ◇ water only control. (b) ■ 0.20% w/v H_2O_2; □ 0.10% w/v • 0.09% w/v; ○ 0.08% w/v; ▲ 0.07% w/v; △ 0.06% w/v; ♦ 0.05% w/v; ◇ catalyst only control. Please refer to the online version of this manuscript for colour figures.

were centrifuged for 5 min at 887 g before the extracellular ATP (upper layer) and intracellular ATP (lower layer) were measured using a FLAA KT assay kit (Sigma Aldrich, UK). Luminescence was measured with an Optocomp 1 luminometer (MGM Instruments, CT, USA), and background luminescence was subtracted. Untreated controls were included. ATP concentrations were determined using a standard curve (Supplementary Material, Fig. S1).

Membrane potential

The membrane potential in the presence of 0.2% H_2O_2 ± 3 g of PAN catalyst was determined using an adapted method from Fisher and Phillips (2009). Leachate samples of 0.2% H_2O_2 with 3 g of PAN catalyst were used for treatment to avoid interference of the solid catalyst substrate with fluorescence. Leachate samples were prepared by incubating 3 g of PAN catalyst and 0.2% H_2O_2 in 75 ml of distilled water at room temperature for 1 h with stirring.

An overnight culture of *E. coli* in BHI broth was washed twice (20 min; 6738 g) in 50 mmol L^{-1} potassium HEPES buffer with 1 mmol L^{-1} magnesium sulphate (pH 7; Fisher Scientific, UK) and diluted to an OD_{600} of 1.0. Membrane potential was measured by adding 30 μL of the cell suspension to 2 mL^{-1} of HEPES buffer containing 5 μmol L^{-1} 3,3-diproylthiacarbocyanine (DPTC) (Sigma-Aldrich, UK). Membrane potential was monitored using a fluorometer (excitation 355 nm, emission 405 nm; Perkins Elmer, UK). Once fluorescence readings had stabilized, cells were energized with 15 mmol L^{-1} glucose (final concentration), followed by 1 nmol L^{-1} nigericin (final concentration; Sigma-Aldrich, UK) after equilibrium to neutralize the membrane pH gradient. After 4 min, 0.2% w/v H_2O_2 ± 3 g of PAN catalyst leachate were added, and the fluorescence was continually measured for 30 min. Water only and 3 g of catalyst leachate in 75 mL of water only treatments were included as negative controls, and valinomycin (1 nmol final concentration) was used as a positive control.

Intracellular pH

Changes in intracellular pH in the presence of 0.2% H_2O_2 ± 3 g of PAN catalyst were determined using an adapted method from Fisher and Phillips (2009).

An overnight culture of *E. coli* in BHI broth was washed twice (20 min; 6738 g) and resuspended in 50 mmol L^{-1} HEPES buffer (pH 7) to an OD_{600} of 1.0. The cell suspensions were incubated for 10 min at 30°C with 1.5 μmol L^{-1} 5(6)-carboxyflurescein diacetate n-succinimidyl ester (CDSE) (Sigma-Aldrich, UK), washed twice in 50 mmol L^{-1} potassium phosphate (Fisher, UK) buffer (pH 5.81) to remove unconjugated CDSE, and incubated for 30 min at 30°C with 10 mmol L^{-1} glucose. A 30 μL sample of the test cell suspension was added to 3 mL of phosphate buffer (pH 5.81), and the fluorescence was measured using a fluorometer (Perkins Elmer, UK) at an emission of 525 nm and an excitation of 490 nm (intracellular pH) or 440 nm (extracellular pH). The 0.2% w/v H_2O_2 ± 3 g PAN catalyst was then added, and fluorescence was monitored again after 15 min of contact. Intracellular and extracellular pH were determined from fluorescence units using standard curves generated with untreated *E. coli* (Supplementary Material, Fig. S2), and the change in intracellular pH was calculated according to Equation (1):

$$\textit{Change in intracellular pH} = \textit{Intracellular pH} - \textit{Extracellular pH}. \quad (1)$$

Statistical analysis

All investigations were conducted in triplicate ($n = 3$). Viable counts were performed with technical duplicates. Student's *t*-tests were conducted using Microsoft Excel to determine significant differences ($P \leq 0.05$) in $\log_{10}$ CFU mL^{-1} survival of *E. coli* between conditions and treatment times after exposure to sublethal concentrations of H_2O_2 alone (0.2% w/v) and with 3 g of catalyst (0.09% w/v). Significant differences ($P \leq 0.05$) in membrane permeability, membrane potential, nucleic acid leakage, ATP leakage, and intracellular pH between 0.2% (w/v) H_2O_2 ± 3 g of catalyst were also determined by Student's *t*-tests using Microsoft Excel.

Results

Sub-lethal concentrations of H_2O_2

H_2O_2 was not significantly antimicrobial ($P > 0.05$) against *E. coli* in the absence of 3 g of PAN catalyst up to 0.20% w/v, where 8.30 ± 0.20 $\log_{10}$ CFU mL^{-1} were recovered after 60 min of exposure (Fig. 1a). In the presence of 3 g of PAN catalyst, the sub-lethal concentration of H_2O_2 was reduced to 0.09%, with 8.48 ± 0.16 $\log_{10}$ CFU mL^{-1} survival after 60 min of treatment ($P > 0.05$; Fig. 1b). The sub-lethal concentrations of 0.20% H_2O_2 alone and 0.09% H_2O_2 + 3 g of

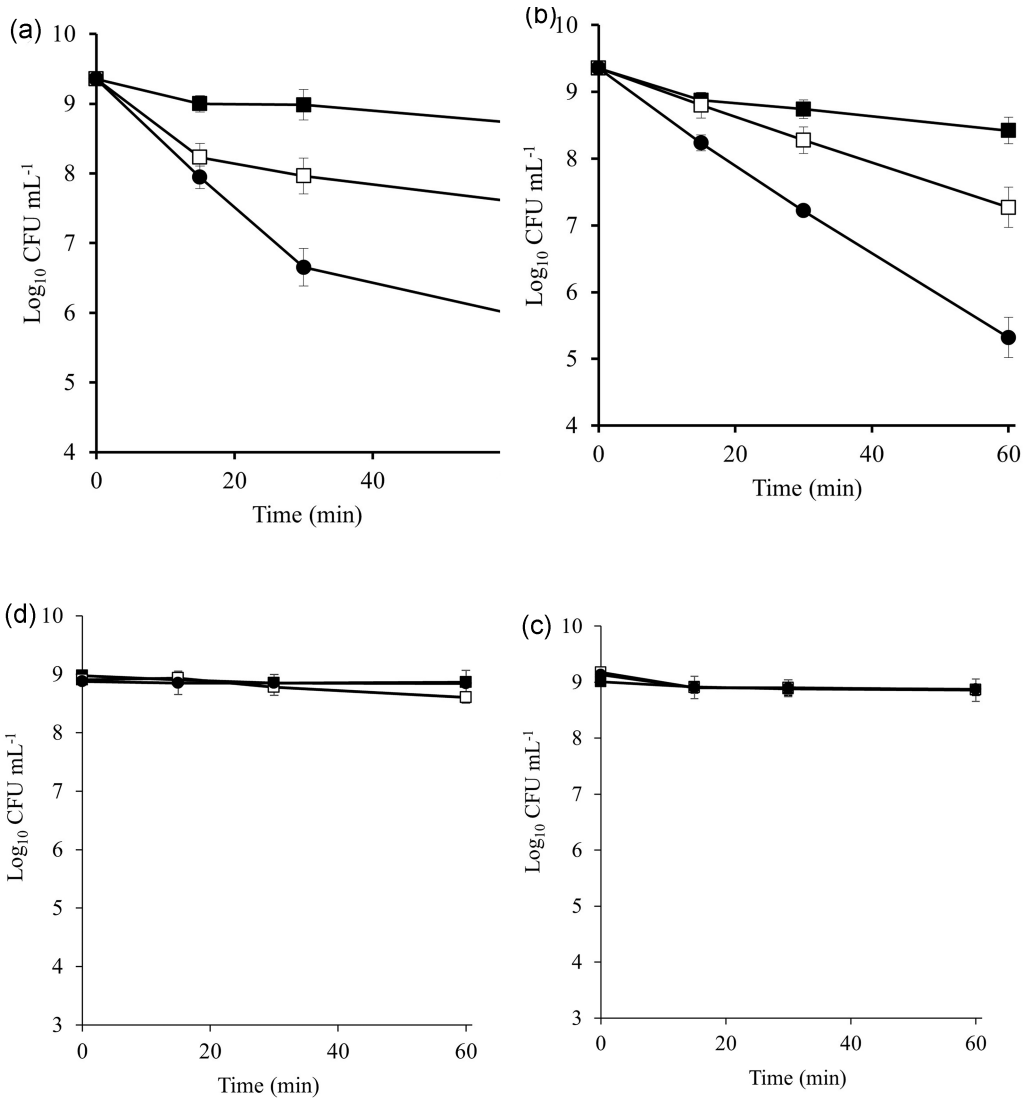

Figure 2. Determination of the type of sub-lethal injury against *E. coli* (8.90 $\log_{10}$ CFU mL^{-1}) log10 CFU/ml recovery by (a) 0.20% w/v H_2O_2 and (b) 0.09% w/v H_2O_2 and 3 g PAN catalyst, (c) water only, and (d) water + 3 g PAN catalyst only (mean, $n = 3 \pm$ SD). ■ TSAYE; • TSAYE + SC; □ TSAYE + BS. Catalyst [Fe] = 16.8 mg g^{-1} (0.30 mmol g^{-1}).

PAN catalyst were used for further investigation of the type of sub-lethal injury to *E. coli*.

Determination of sub-lethal injury

Sublethal concentrations of H_2O_2 (0.20% w/v) significantly ($P < 0.05$) decreased recovery on TSAYE + SC (6.65 $\log_{10}$ CFU mL^{-1}) and TSAYE + BS (7.60 $\log_{10}$ CFU mL^{-1}) compared to TSAYE alone (8.48 $\log_{10}$ CFU mL^{-1}) (Fig. 2a). This suggests a loss of cytoplasmic membrane and outer membrane function, respectively. Similarly, H_2O_2 (0.09% w/v) + 3 g of PAN catalyst significantly ($P \leq 0.05$) reduced the tolerance of *E. coli* to sodium chloride and bile salts; the recovery of *E. coli* was 7.22 $\log_{10}$ CFU mL^{-1} on TSAYE + SC after 30 min of treatment and 7.27 $\log_{10}$ CFU mL^{-1} on TSAYE + BS after 60 min of treatment, compared to 8.48 $\log_{10}$ CFU mL^{-1} on TSAYE alone (Fig. 2b). Water or a 3 g PAN catalyst alone did not reduce the viability of *E. coli* on TSAYE + SC or TSAYE + BS (Fig. 2c and d).

The mechanisms of action of the catalyst were further explored by directly comparing the effects of 0.2% H_2O_2 with and without the 3 g PAN catalyst upon membrane permeability, membrane potential, nucleic acid leakage, ATP leakage, and intracellular pH.

Membrane permeability

Treatment of *E. coli* with 0.2% w/v H_2O_2 alone increased cell membrane permeability by 1.34-fold after 5 min and 1.51-fold after 30 min (Table 1). Exposure to 0.2% H_2O_2 and 3 g PAN catalyst significantly increased ($P \leq 0.05$) cell membrane permeability compared to H_2O_2 alone after 5 min (1.51-fold); no significant difference ($P > 0.05$) was observed after 30 min (1.52-fold; Table 1).

Nucleic acid leakage

The OD_{260nm} of untreated controls did not differ significantly ($P > 0.05$) between 0 and 60 min (Fig. 3). There was a significant increase ($P < 0.05$) in OD_{260nm} after 40–60 min of treatment with 0.2% w/v H_2O_2 compared to the control, indicating a loss of nucleic acids from the cells. H_2O_2 and 3 g of PAN

Table 1. Membrane permeability of *E. coli* (OD_{620nm} = 1.0) treated with 0.2% w/v H_2O_2 ± 3 g PAN catalyst as determined by NPN uptake (mean, $n = 3 \pm SD$).

Sample	Fluorescence value, a.u. (Fold change)			
	0 min	5 min	15 min	30 min
NPN, H_2O_2 and Catalyst only (Background)*	52.49 ± 0.12	–	–	–
NPN + *E. coli* only†	352.22 ± 6.35	–	–	–
0.2% w/v H_2O_2†	–	472.40 ± 4.41 (1.34)	532.56 ± 1.67 (1.51)	533.23 ± 0.75 (1.52)
0.2% w/v H_2O_2 and Catalyst†	–	531.32 ± 2.58 (1.51)	534.27 ± 1.94 (1.52)	535.78 ± 0.41 (1.52)

*Fluorescence values (a.u.) after background subtracted.
†Fluorescence values for H_2O and 0.2% w/v H_2O_2 + 3 g PAN catalyst alone = 0.00 ± 0.00.
Catalyst [Fe] = 16.8 mg g^{-1} (0.30 mmol g^{-1}).

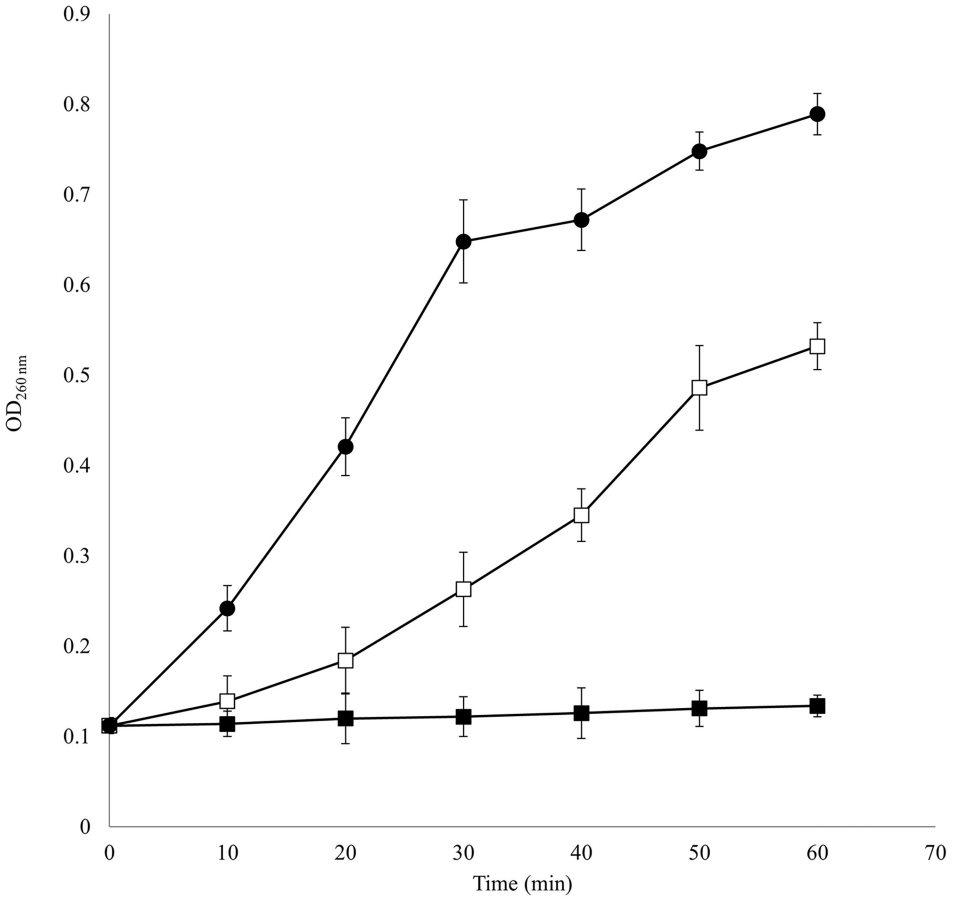

Figure 3. Loss of nucleic acid (OD_{260nm}) after exposure to 0.2% w/v H_2O_2 ± 3 g PAN catalyst against *E. coli* (mean, $n = 3 \pm SD$). ■ Untreated control; □ 0.2% w/v H_2O_2 • 0.2% w/v H_2O_2 + 3 g PAN catalyst. Catalyst [Fe] = 16.8 mg g^{-1} (0.30 mmol g^{-1}).

catalyst further increased OD_{260nm} at 20–60 min, which was statistically significant ($P < 0.05$) compared to H_2O_2 alone.

Intra- and extracellular ATP

Loss of intracellular ATP from 9.0 ± 0.89 nmol to undetectable levels occurred when *E. coli* was exposed to H_2O_2 ± 3 g PAN catalyst at 10 min, whereas with 0.2% w/v H_2O_2 alone this dropped to undetectable levels at 12 min (Fig. 4). However, extracellular ATP showed no significant difference ($P > 0.05$) compared to controls and remained at 0 nmol, suggesting that the intracellular ATP did not leak into the extracellular environment (Fig. 4).

Membrane potential

The PAN catalyst and 0.2% w/v H_2O_2 alone did not fluoresce (0.000 ± 0.000 a.u.). When 0.2% w/v H_2O_2 was added, the membrane potential of the cells was reduced from 0.041 to 0.027 a.u. at 15 min (Fig. 5). When the PAN catalyst and 0.2% w/v H_2O_2 were added, there was a more rapid and overall significantly greater ($P \leq 0.05$) loss of membrane potential (0.015 a.u. at 15 min) compared to 0.2% w/v H_2O_2 alone. The membrane potential of the water-only and catalyst-only controls remained relatively stable over time, with a reduction of 0.004–0.005 a.u. between the addition of water or catalyst (4 min) and 30 min.

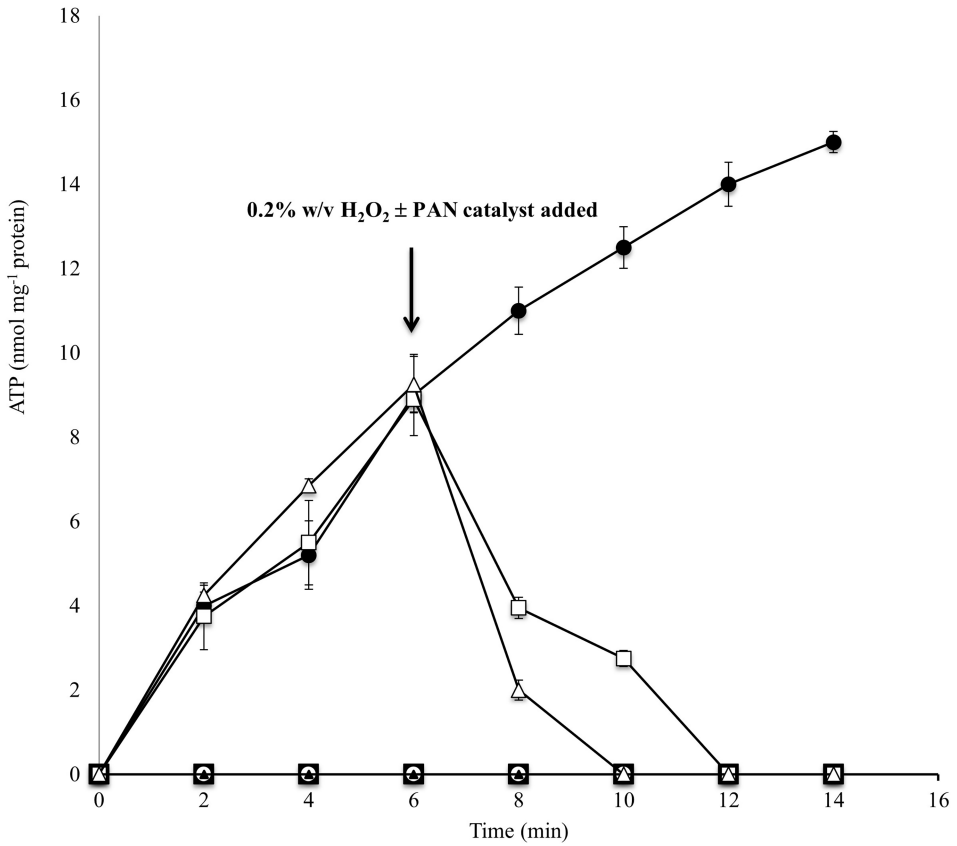

Figure 4. Intra- and extracellular ATP concentration of *E. coli* and 0.2% w/v H_2O_2 ± 3 g PAN catalyst (mean, $n = 3$ ± SD). ■ Extracellular ATP control; • intracellular ATP control; ○ extracellular ATP, 0.2% w/v H_2O_2; □ intracellular ATP, 0.2% w/v H_2O_2; ▲ extracellular ATP, 0.2% w/v H_2O_2 + 3 g PAN catalyst; △ intracellular ATP, 0.2% w/v H_2O_2 + 3 g PAN catalyst. Catalyst [Fe] = 16.8 mg g^{-1} (0.30 mmol g^{-1}).

Change in intracellular pH

After 15 min of exposure to 0.2% w/v H_2O_2 alone, intracellular pH decreased from 6.39 to 5.30 and extracellular pH decreased from 5.61 to 5.29 (Table 2). Addition of 3 g of PAN catalyst resulted in a significantly ($P \leq 0.05$) greater decrease in intracellular pH (6.43–4.75) and extracellular pH (5.58–4.75) compared to H_2O_2 alone (Table 2).

Discussion

The cell membrane is a target for many biocidal agents, and changes can occur in both membrane structure and function (Jones and Joshi 2021). H_2O_2 also enters the cell through porins and diffusion through the outer membrane (Feng et al. 2020), where it causes oxidative damage to DNA, lipids, and proteins (Dhawale et al. 2021). In accordance with previous research (Boateng et al. 2011, Price et al. 2013), this study demonstrated that H_2O_2 ± 3 g PAN catalyst resulted in sub-lethal injury to *E. coli*, whereby viability was not decreased during 60 min of exposure, yet tolerance to sodium chloride and bile salts was decreased (Figs 2 and 3). An increase in the sensitivity of *E. coli* to sodium chloride following exposure to H_2O_2 (Fig. 2) suggests potential cytoplasmic membrane damage due to impairment of osmotic homeostasis (Carson et al. 2002). Bile salt tolerance was also decreased following H_2O_2 exposure (Fig. 2), albeit to a lesser extent than sodium chloride. Efflux pumps and glycolipids such as lipopolysaccharide in the outer membrane confer resistance to bile salts (Urdaneta and Casadesús 2017); therefore, increased sensitivity of *E. coli* infers outer membrane damage. H_2O_2 also increased the permeability of the *E. coli* cell membrane, as demonstrated by increased NPN uptake (Table 1) and leakage of 260 nm-absorbing cellular material (Fig. 3). Similarly, Feng et al. (2020) demonstrated an increase in membrane permeability in *E. coli* treated with 10 ppm H_2O_2 over 180 min, without a decrease in viability over the same time period. H_2O_2 is a strong oxidizing agent (Jones and Joshi 2021), which can cause lipid peroxidation in the *E. coli* cell envelope and subsequently alter membrane permeability (Feng et al. 2020, Kim and Lee 2021). Cell membrane damage was also evidenced by the loss of membrane potential (Fig. 5), which has been associated with membrane lipid peroxidation by H_2O_2 and OH• (Kim and Lee 2021). Both membrane permeabilization and depolarization were more pronounced in the presence of the PAN catalyst. This may be attributed to increased production of OH• radicals by the Fenton reaction in the presence of ferric ions within the catalyst, which more effectively oxidize biological molecules than H_2O_2 (Collin 2019). A similar potentiation of the biocidal activity of H_2O_2 has been observed with titanium and copper catalysts (Nguyen et al. 2013, Wiedmer et al. 2017), hence the lower sub-lethal concentration of H_2O_2 needed when the PAN catalyst is present.

Depletion of intracellular ATP was observed after H_2O_2 ± PAN catalyst treatment, which was not attributed to leakage into the extracellular environment (Fig. 4). These findings may be the result of the termination of ATP synthesis or an increase in ATP hydrolysis (Fisher and Phillips 2009).

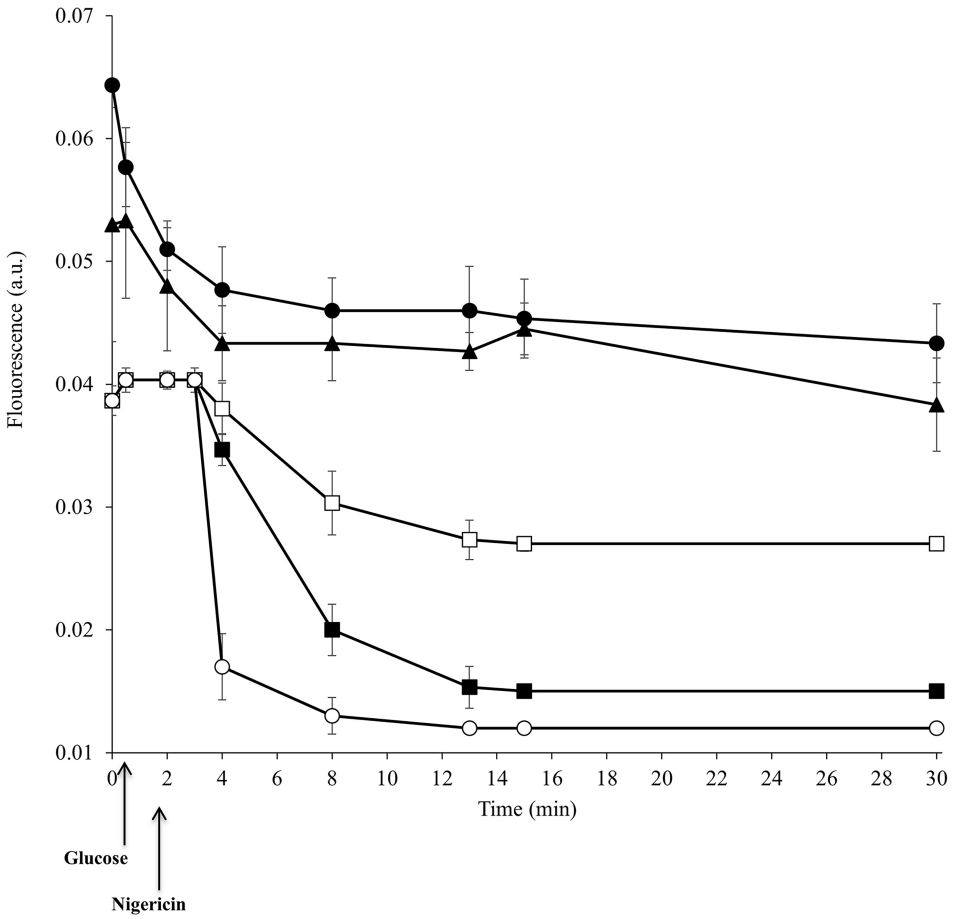

Figure 5. Change in membrane potential after the addition of 0.2% w/v H_2O_2 ± 3 g PAN catalyst or 1 nmol L^{-1} valinomycin against *E. coli* (mean, $n = 3 \pm$ SD). ■ 0.2% w/v H_2O_2 + 3 g PAN catalyst; □ 0.2% w/v H_2O_2; ○ 1 nmol L^{-1} valinomycin; ▲water only control; ● catalyst only control. Catalyst [Fe] = 16.8 mg g^{-1} (0.30 mmol g^{-1}).

Table 2. Change in intracellular and extracellular pH following treatment with 0.2% H_2O_2 ± 3 g PAN catalyst ($n = 3 \pm$ SD).

	Intracellular pH		Extracellular pH	
Sample	Fluorescence 490 nm (a.u.)*	pH	Fluorescence 440 nm (a.u.)*	pH
Buffer only (pH 5.81)	0.624 ± 0.036	–	1.276 ± 0.005	–
Blank H_2O	0.092 ± 0.001	–	0.844 ± 0.007	–
Pre-treatment control	81.492 ± 0.033	6.39 ± 0.03	11.148 ± 0.058	5.61 ± 0.06
0.2% H_2O_2	45.867 ± 0.086	5.27 ± 0.09	9.032 ± 0.045	5.29 ± 0.05
Pre-treatment control	82.063 ± 0.146	6.43 ± 0.15	11.107 ± 0.043	5.58 ± 0.05
0.2% H_2O_2 + Catalyst	36.462 ± 0.565	4.75 ± 0.57	6.734 ± 0.205	4.75 ± 0.21

*Fluorescence values (a.u.) after background subtracted.
Catalyst [Fe] = 16.8 mg g^{-1} (0.30 mmol g^{-1}).

Transmembrane ATP synthases produce ATP using proton or sodium motive force, suggesting the latter occurred as a result of membrane depolarization (Benarroch and Asally 2020). Previous studies have also reported damage to ATP synthase proteins themselves by reactive oxygen species (Collin 2019).

A change in internal pH could also limit ATP synthesis, as changes in pH >3.0 units (Dimroth et al. 2000) may denature ATP synthases, while the loss of ions could impact proton motive force and ATPase activity (Cox et al. 2000, Rao et al. 2008). In the presence of the H_2O_2 ± PAN catalyst, there was also a complete disruption of intracellular pH homeostasis (Table 2). Intracellular pH decreased from 6.39–6.43 to 5.27–4.75—equal to that of the external environment—while the external environment itself showed a decrease in pH, particularly when the PAN catalyst was present (pH 4.75), in accordance with previous findings (Boateng et al. 2011). *E. coli* maintains pH homeostasis via ion channels and is known to respond rapidly to changes in intracellular pH (Slonczewski et al. 2009); thus, a loss of pH homeostasis suggests the occurrence of cytoplasmic membrane damage by H_2O_2 ± PAN catalyst. Perturbation of pH homeostasis was also associated with DNA damage in *E. coli* treated with nalidixic acid (Booth et al. 2020); considering that H_2O_2 is known to cause DNA damage (Dhawale et al. 2021), this could also contribute to loss of pH homeostasis, and further

investigation on the possible roles of each mechanism of damage is warranted.

This study demonstrated that a novel PAN catalyst potentiates the antimicrobial activity of H_2O_2 against *E. coli,* reducing inhibitory concentrations. The cell membrane is a major target of H_2O_2, resulting in increased permeability and depletion of membrane potential, intracellular ATP, and pH homeostasis; these effects were more pronounced in the presence of the PAN catalyst. The increased antimicrobial activity of the PAN catalyst may be due to leached iron generating OH• via the Fenton reaction, and a possible reactive iron species. Further analysis of the iron species and its antimicrobial properties would need to be undertaken in order to fully determine the PAN catalyst's antimicrobial activity, as well as further investigations into the MOA of the H_2O_2 ± PAN catalyst system.

Supplementary data

Supplementary data is available at *JAMBIO Journal* online.

Conflict of interest

No conflict of interest declared.

Funding

We wish to thank De Montfort University for providing funding for this research via their doctoral training grant programme.

Author contributions

S. L. Sewell contributed to the experimental design, collection, analysis, and interpretation of the data, the manuscript drafting and review, and the decision to submit the report for publication. K. Laird contributed to the experimental design, analysis and interpretation of the data, manuscript review, and decision to submit the report for publication. K. D. Huddersman and S. E. Walsh contributed to project supervision, experimental design, manuscript drafting, and review. L. Owen contributed to the collection, analysis, and interpretation of the data, manuscript drafting and review, and the decision to submit the report for publication.

Data availability

All data generated or analysed during this study are included in this published article.

References

Agashe P, Kuzminov A. Nitric oxide precipitates catastrophic chromosome fragmentation by bolstering both hydrogen peroxide and Fe (II) fenton reactants in *E. Coli*. *J Biol Chem* 2022;**298**:101825. https://doi.org/10.1016/j.jbc.2022.101825

Benarroch JM, Asally M. The microbiologist's guide to membrane potential dynamics. *Trends Microbiol* 2020;**28**:304–14. https://doi.org/10.1016/j.tim.2019.12.008

Boateng MK, Price SL, Huddersman KD *et al*. Antimicrobial activities of hydrogen peroxide and its activation by a novel heterogeneous Fenton's-like modified PAN catalyst. *J Appl Microbiol* 2011;**111**:1533–43. https://doi.org/10.1111/j.1365-2672.2011.05158.x

Booth JA, Špírek M, Lobie TA *et al*. Antibiotic-induced DNA damage results in a controlled loss of pH homeostasis and genome instability. *Sci Rep* 2020;**10**:1–18. https://doi.org/10.1038/s41598-020-76426-2

British Standards Institution. *BS EN 1040:2005—Chemical disinfectants and antiseptics. Quantitative suspension test for the evaluation of basic bactericidal activity of chemical disinfectants and antiseptics. Test method and requirements (phase 1)*. London: British Standards Institution, 2005.

Carson CF, Mee BJ, Riley TV. Mechanism of action of *Melaleuca alternifolia* (tea tree) oil on *Staphylococcus aureus* determined by time-kill, lysis, leakage, and salt tolerance assays and electron microscopy. *Antimicrob Agents Chemother* 2002;**46**:1914–20. https://doi.org/10.1128/AAC.46.6.1914-1920.2002

Chen CZ, Cooper SL. Interaction between dendrimer biocides and bacterial membranes. *Biomaterials* 2002;**23**:3359–68. https://doi.org/10.1016/S0142-9612(02)00036-4

Cheng X, Zu L, Jiang Y *et al*. A titanium-based photo-fenton bifunctional catalyst of mp-mxene/TiO 2—x nanodots for dramatic enhancement of catalytic efficiency in advanced oxidation processes. *Chem Commun* 2018;**54**:11622–5. https://doi.org/10.1039/C8CC05866K

Collin F. Chemical basis of reactive oxygen species reactivity and involvement in neurodegenerative diseases. *Int J Mol Sci* 2019;**20**:2407. https://doi.org/10.3390/ijms20102407

Cox SD, Mann CM, Markham JL *et al*. The mode of antimicrobial action of the essential oil of *Melaleuca alternifolia* (tea tree oil). *J Appl Microbiol* 2000;**88**:170–5. JAMBIO

Dhawale A, Bindal G, Rath D *et al*. DNA repair pathways important for the survival of *Escherichia coli* to hydrogen peroxide mediated killing. *Gene* 2021;**768**:145297. https://doi.org/10.1016/j.gene.2020.145297

Dimroth P, Kaim G, Matthey U. Crucial role of the membrane potential for ATP synthesis by F (1) F (o) ATP synthases. *J Exp Biol* 2000;**203**:51–59. https://doi.org/10.1242/jeb.203.1.51

Fisher K, Phillips C. The mechanism of action of a citrus oil blend against *Enterococcus faecium* and *Enterococcus faecalis*. *J Appl Microbiol* 2009;**106**:1343–9. https://doi.org/10.1111/j.1365-2672.2008.04102.x

Feng L, Peillex-Delphe C, Lü C *et al*. Employing bacterial mutations for the elucidation of photo-fenton disinfection: focus on the intracellular and extracellular inactivation mechanisms induced by UVA and H_2O_2. *Water Res* 2020;**182**:116049. https://doi.org/10.1016/j.watres.2020.116049

Gabriel MM, McAnally C, Chen H *et al*. Hydrogen peroxide disinfecting solution for gas permeable contact lenses: a review of the antimicrobial efficacy, compatibility, and safety performance of a one-step lens care system. *Clinical Optometry* 2021;**13**:7. https://doi.org/10.2147/OPTO.S280046

Huddersman K, Walsh SE. Antimicrobial Agent. Patent #US8513303 B2, published August 20, 2013.

Ishtchenko VV, Vitkovskaya RF, Huddersman K. Part 1. Production of a modified PAN fibrous catalyst and its optimisation towards the decomposition of hydrogen peroxide. *Appl Catal, A* 2003;**242**:123–37. https://doi.org/10.1016/S0926-860X(02)00511-2

Jones IA, Joshi LT. Biocide use in the antimicrobial era: a review. *Molecules* 2021;**26**:2276. https://doi.org/10.3390/molecules26082276

Kilvington S, Winterton L. Fibrous catalyst-enhanced *Acanthamoeba* disinfection by hydrogen peroxide. *Optom Vis Sci* 2017;**94**:1022–8. https://doi.org/10.1097/OPX.0000000000001126

Kim H, Lee DG. Contribution of SOS genes to H_2O_2-induced apoptosis-like death in *Escherichia coli*. *Curr Genet* 2021;**67**:969–80. https://doi.org/10.1007/s00294-021-01204-0

Lineback CB, Nkemngong CA, Wu ST *et al*. Hydrogen peroxide and sodium hypochlorite disinfectants are more effective against *Staphylococcus aureus* and *Pseudomonas aeruginosa* biofilms than quaternary ammonium compounds. *Antimicrob Resist Infect Control* 2018;**7**:1–7. https://doi.org/10.1186/s13756-018-0447-5

Linley E, Denyer SP, Mcdonnell G *et al*. Use of hydrogen peroxide as a biocide: new consideration of its mechanisms of biocidal action. *J Antimicrob Chemother* 2012;**67**:1589–96. https://doi.org/10.1093/jac/dks129

McEvoy B, Rowan NJ. Terminal sterilization of medical devices using vaporized hydrogen peroxide: a review of current methods and emerging opportunities. *J Appl Microbiol* 2019;**127**:1403–20. https://doi.org/10.1111/jam.14412

Meyerstein D. Re-examining fenton and fenton-like reactions. *Nat Rev Chem* 2021;**5**:595–7. https://doi.org/10.1038/s41570-021-00310-4

Miles AA, Misra SS. The estimation of the bactericidal power of the blood. *J Hyg* 1938;**38**:732–49.

Möller MN, Cuevasanta E, Orrico F *et al*. Diffusion and transport of reactive species across cell membranes. In: Trostchansky A, Rubbo H . (eds), *Bioactive Lipids in Health and Disease*, Vol. **1127**. Cham: Springer, 2019, 3–19.

Nguyen TT, Park HJ, Kim JY *et al*. Microbial inactivation by cupric ion in combination with H_2O_2: role of reactive oxidants. *Environ Sci Technol* 2013;**47**:13661–7. https://doi.org/10.1021/es403155a

Price SL, Huddersman KD, Shen J *et al*. Mycobactericidal activity of hydrogen peroxide and a novel heterogeneous fentons-like modified PAN catalyst system. *Lett Appl Microbiol* 2013;**56**:83–87. https://doi.org/10.1111/lam.12010

Rao SP, Alonso S, Rand L *et al*. The protonmotive force is required for maintaining ATP homeostasis and viability of hypoxic, nonreplicating *Mycobacterium tuberculosis*. *Proc Natl Acad Sci* 2008;**105**:11945–50. https://doi.org/10.1073/pnas.0711697105

Slonczewski JL, Fujisawa M, Dopson M *et al*. Cytoplasmic pH measurement and homeostasis in bacteria and archaea. *Adv Microbial Physiol* 2009;**55**:1–79. https://doi.org/10.1016/S0065-2911(09)05501-5

Somolinos M, Garcia D, Condon S *et al*. Inactivation of *Escherichia coli* by citral, *J Appl Microbiol* 2009;**108**:1928–39. https://doi.org/10.1111/j.1365-2672.2009.04597.x

Urdaneta V, Casadesús J. Interactions between bacteria and bile salts in the gastrointestinal and hepatobiliary tracts. *Front Med* 2017;**4**:163. https://doi.org/10.3389/fmed.2017.00163

Výrostková J, Pipová M, Semjon B *et al*. Antibacterial effects of hydrogen peroxide and caprylic acid on selected foodborne bacteria. *Pol J Vet Sci* 2020;**23**:439–46.

Walter M, Schenkeveld WD, Geroldinger G *et al*. Identifying the reactive sites of hydrogen peroxide decomposition and hydroxyl radical formation on chrysotile asbestos surfaces. *Part Fibre Toxicol* 2020;**17**:3. https://doi.org/10.1186/s12989-019-0333-1

Wiedmer D, Petersen FC, Lönn-Stensrud J *et al*. Antibacterial effect of hydrogen peroxide-titanium dioxide suspensions in the decontamination of rough titanium surfaces. *Biofouling* 2017;**33**:451–9. https://doi.org/10.1080/08927014.2017.1322585

Supplementary Material: The antimicrobial mechanisms of action of a Novel Heterogeneous Fenton's-like Catalyst

Supplementary Tables

Table S1: Efficacy and toxicity of catalase as a neutraliser against H_2O_2 ± PAN catalyst (mean, n=3 ± S.D).

Condition	**Log_{10} CFU mL^{-1}**
Initial count	8.90 ± 0.15
Neutraliser efficacy (0.4% H_2O_2)	8.79 ± 0.21
Neutraliser toxicity	8.57 ± 0.39
PAN catalyst toxicity ([Fe] = 16.8mg/g (0.30mmol/g)	8.93 ± 0.12

Table S2: Maximum non-inhibitory concentration of sodium chloride and bile salts against *E. coli* (mean, n=3 ± SD).

Concentration of bile salts	**Log_{10} CFU mL^{-1}**
TSAYE + 0.1% bile salts	8.92 ± 0.19
TSAYE + 0.2% bile salts	8.79 ± 0.21
TSAYE + 0.3% bile salts	7.14 ± 0.47
TSAYE + 0.4% bile salts	6.37 ± 0.35
TSAYE + 2.0% sodium chloride	8.88 ± 0.21
TSAYE + 3.0% sodium chloride	8.77 ± 0.27
TSAYE + 4.0% sodium chloride	8.71 ± 0.25
TSAYE + 5.0% sodium chloride	7.79 ± 0.32

Supplementary Figures

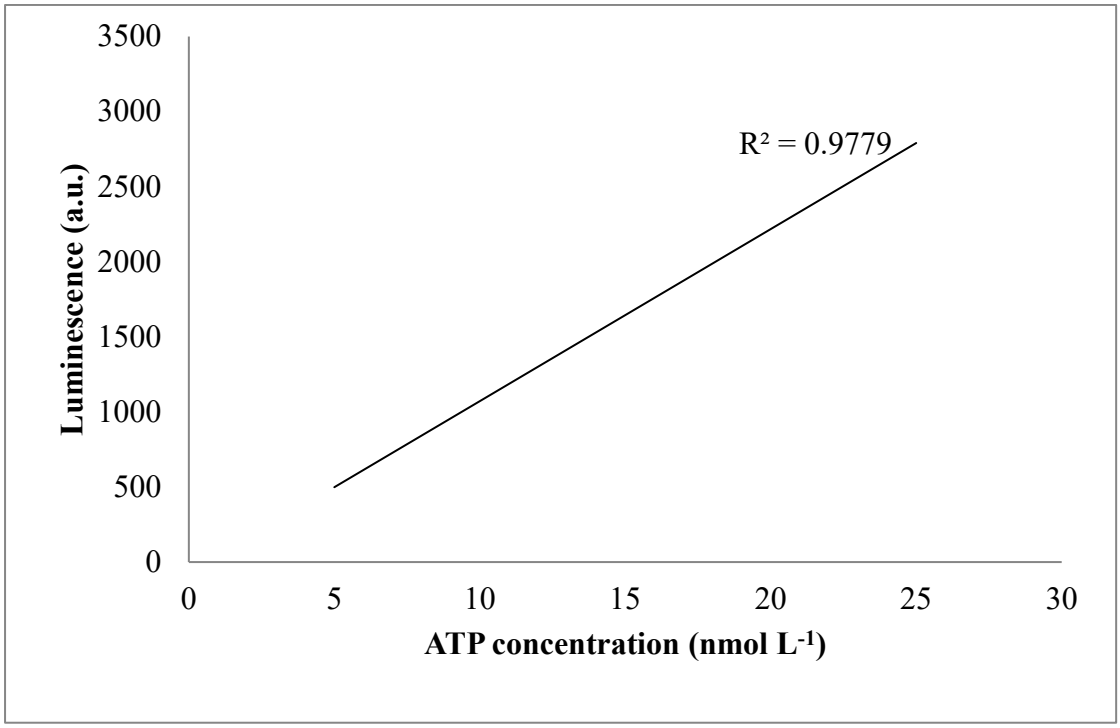

Figure S1:1 Standard curve of ATP concentration.

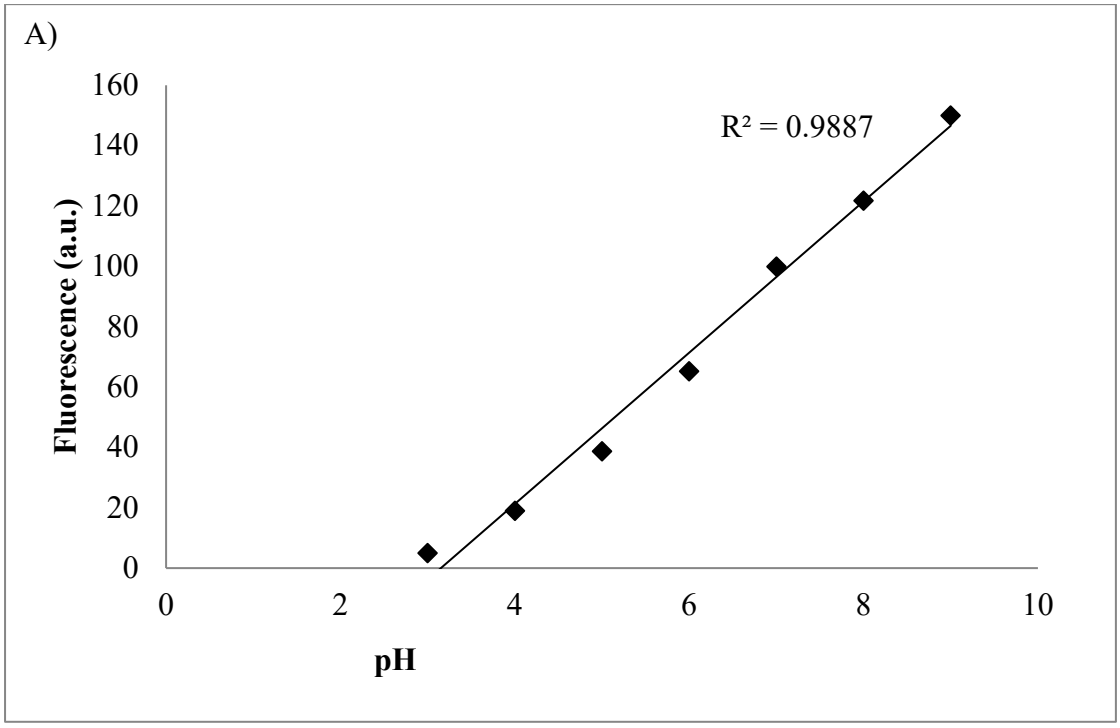

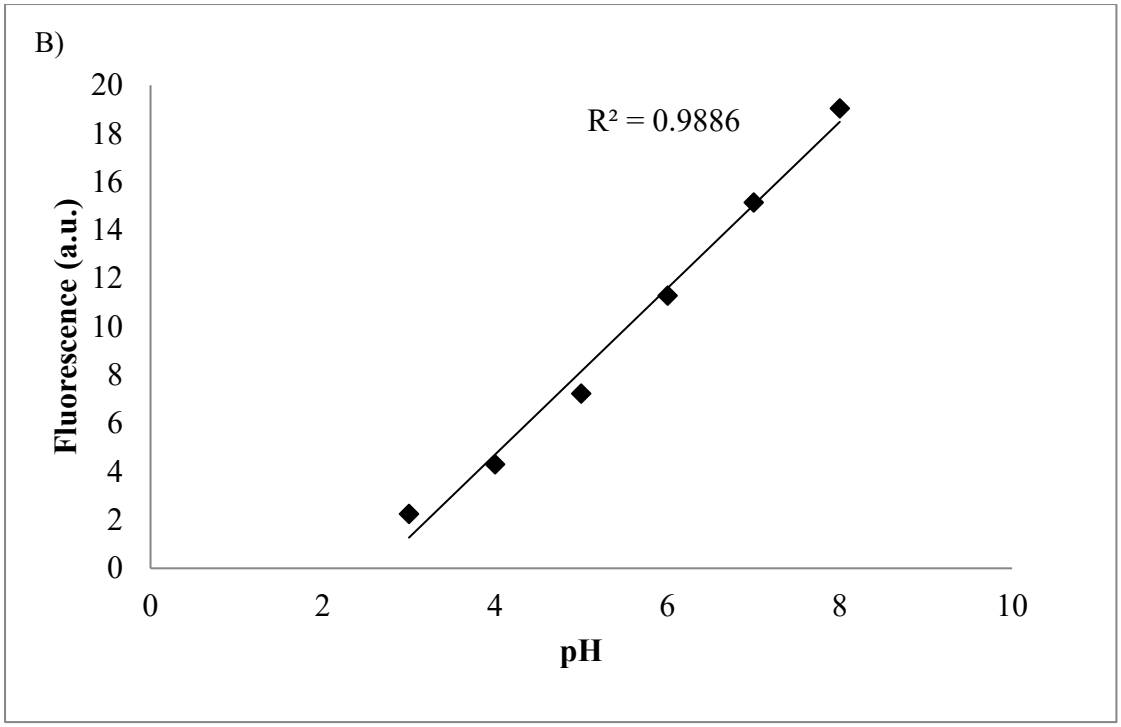

Figure S2: Standard curves for a) modified intracellular pH and b) modified extracellular pH in *E. coli.*